Synthesis of cobalt sulfide multi-shelled nanoboxes with precisely controlled two to five shells for sodium-ion batteries

Wang, Xiao; Chen, Ye; Fang, Yongjin; Zhang, Jintao; Gao, Shuyan; Lou, David Xiong Wen

2019

Wang, X., Chen, Y., Fang, Y., Zhang, J., Gao, S., & Lou, D. X. W. (2019). Synthesis of cobalt sulfide multi-shelled nanoboxes with precisely controlled two to five shells for sodium-ion batteries. Angewandte Chemie International Edition, 58(9), 2675-2679. doi:10.1002/ange.201812387

https://hdl.handle.net/10356/138599

https://doi.org/10.1002/ange.201812387

Synthesis of Cobalt Sulfide Multi-shelled Nanoboxes with Precisely Controlled 2-5 Shells for Sodium-Ion Batteries

*Xiao Wang, Ye Chen, Yongjin Fang, Jintao Zhang, Shuyan Gao, and Xiong Wen (David) Lou**

[*]Y. Chen, Prof. S. Y. Gao
School of Materials Science and Engineering, Henan Normal University, Xinxiang, Henan 453007, P.R. China. Email: shuyangao@htu.cn

Dr. X. Wang, Dr. Y. Fang, J. T. Zhang, Prof. X. W. Lou
School of Chemical and Biomedical Engineering, Nanyang Technological University, 62 Nanyang Drive, Singapore, 637459, (Singapore)
Email: xwlou@ntu.edu.sg; Webpage: http://www.ntu.edu.sg/home/xwlou/

Abstract

We report the synthesis of cobalt sulfide multi-shelled nanoboxes through metal-organic framework (MOF)-engaged complex anion conversion and exchange processes. The polyvanadate ions transformed from metavanabate ions in alkaline media first react with cobalt-based zeolitic imidazolate framework-67 (ZIF-67) nanocubes to form ZIF-67/cobalt polyvanadate yolk-shelled particles. Afterwards, the as-formed ZIF-67/cobalt polyvanadate yolk-shelled particles are gradually converted to cobalt divanadate multi-shelled nanoboxes by a solvothermal treatment under neutral condition. The number of shells in the range of 2 – 5 can be easily controlled by varying the temperature. Finally, the cobalt sulfide multi-shelled nanoboxes are produced through the ion-exchange reaction with S^{2-} ions and a subsequent annealing treatment. The as-obtained cobalt sulfide multi-shelled nanoboxes exhibit enhanced sodium storage properties when evaluated as anodes for sodium-ion batteries. For example, a high specific capacity of 438 mAh g^{-1} can be retained after 100 cycles at the current density of 500 mA g^{-1} for the triple-shelled nanoboxes.

Keywords: multi-shelled structures; cobalt sulfide; ion-exchange reaction; sodium-ion battery

The fast depletion of fossil fuels and growing environmental concerns have prompted intense research efforts for the development of clean and sustainable energy storage and conversion technologies. Electrical energy storage devices as one of the most important components in the development of sustainable energy systems have attracted significant research interest.[1-3] Besides lithium-ion batteries (LIBs), sodium-ion batteries (SIBs) have been considered as one promising energy storage alternative because sodium is abundantly available.[2, 4-8] Among the potential negative electrode materials for SIBs, transition metal sulfides (TMSs) are quite attractive because of their rich redox sites, high capacity and enhanced electrical conductivity compared with their oxide counterparts.[9-13] However, practical applications of TMSs are still hindered by the poor rate performance and fast capacity fading due to the low intrinsic electric conductivity, gradually reduced crystallinity and inevitable volume changes during prolonged cycling.

To circumvent these problems, rational design of the structural complexity of active materials has been proved a promising strategy.[9, 14-18] In particular, hollow structures with complex interiors have drawn significant attention owing to their structure-dependant merits. As for sodium storage applications, intricate hollow structures exhibit great advantages over simple hollow architectures.[16, 19-21] Complex hollow particles not only inherit all the advantages of hollow structures, including high surface area, enhanced volume change accommodation and large electrode/electrolyte interface, but also improve weight fraction of active species, thus dramatically enhancing the energy density of the electrode materials.[22] As a result, a variety of electrode materials have been fabricated in the form of multi-shelled hollow structures.[23-31] It is also noted that non-spherical particles might exhibit some advantage for SIBs,[9, 15] owing to their larger surface area compared to spherical counterparts with identical volume. The higher surface area may bring in some important positive effects, such as more abundant active sites and better electrolyte adsorption.[32-33] Despite all these achievements mentioned above, studies on non-spherical multi-shelled particles with precisely controlled number of shells for high-performance SIBs are still rare due to the challenges in synthesis of such multi-shelled particles.

In recently years, hollow structured materials derived from metal-organic frameworks (MOFs) have been intensively investigated in energy-related applications.[6-7, 23-26, 32-34] Given the presence of both thermally and chemically unstable porous frameworks, MOFs can be easily converted to hollow structured materials via pyrolysis or chemical reactions with desirable reagents. Among different transformation methods, ion-exchange reactions have been shown as an effective tool for structural and compositional transformation of MOFs.[8, 24, 35] Therefore, rational design of multi-step ion-exchange strategies may pave the way to construct MOF-derived complex hollow particles, in terms of both shell architecture and chemical composition.

Herein, we report an "ion-conversion-exchange" strategy to synthesize cobalt sulfide multi-shelled nanoboxes (MSNBs) with precisely controlled number of shells for sodium storage. The ion conversion and exchange reactions developed in this work can enable control in both structure and composition of the as-derived particles. We first transform zeolitic imidazolate framework-67 (ZIF-67) nanocubes (NCs) into ZIF-67/cobalt polyvanadate yolk-shell nanocubes (YSNCs) through the ion-exchange reaction between the MOF precursor and polyvanadate ions. Afterwards, the cobalt polyvanadate outer layer can be converted to cobalt divanadate shell during the solvothermal treatment in neutral media. At the same time, the divanadate ions released from the outer shell further react with the inner ZIF-67 core to form cobalt divanadate MSNBs. Finally, the obtained cobalt divanadate multi-shelled particles can be further converted into cobalt sulfide MSNBs though a sulfidation process (**Figure 1**). When applied as anode materials for SIBs, these complex cobalt sulfide MSNBs exhibit excellent electrochemical properties with high specific capacity and excellent cycling stability.

Uniform ZIF-67 NCs with an average particle size of ~800 nm are first synthesized by a previously reported method (**Figure 2**a).[34, 36-37] The as-prepared ZIF-67 NCs are converted to ZIF-67/cobalt polyvanadate YSNCs through an ion-exchange reaction with polyvanadate ions produced from concentrated metavanadate ions under weakly alkaline condition.[38] The field-emission

scanning electron microscope (FESEM) image (Figure 2b) of the sample reveals that the as-derived particles retain the cubic morphology of their MOF precursors. As further elucidated by transmission electron microscope (TEM) observation (Figure 2c), a yolk-shelled structure can be clearly observed. The X-ray diffraction (XRD) characterization indicate that the solid core retains its original crystalline structure of ZIF-67 (Figure S1, Supporting Information). Meanwhile, no other peaks are observed, indicating the amorphous nature of the as-formed cobalt polyvanadate shells. The energy-dispersive X-ray spectroscope (EDX) analysis confirms the existence of the V element in the product (Figure S2, Supporting Information). The elemental mapping images further reveal that the V element exists only in the outer shells of the yolk-shelled particles (Figure 2d). The molar ratio of Co to V in the cobalt polyvanadate shells is further determined to be ~1:2.86 by the EDX analysis of a control sample with completely hollow cobalt polyvanadate nanoshells (Figure S3, Supporting Information). Such a high V/Co molar ratio confirms the formation of cobalt polyvanadate.

The as-obtained ZIF-67/cobalt polyvanadate YSNCs are transformed to cobalt divanadate triple-shelled nanoboxes (TSNBs) through a mild solvothermal process under neutral condition at 50 ºC. The cubic morphology of the sample is still retained after the solvothermal treatment (Figure S4a,e, Supporting information). Triple-shelled nanoboxes can be clearly discerned in the TEM images (**Figure 3**a,b). As shown in the XRD pattern (Figure S5, Supporting Information), the as-formed cobalt divanadate particles are also amorphous. Compared with the sole cobalt polyvanadate nanoshells, the Co/V/O molar ratio of cobalt divanadate TSNBs greatly increases to ~1:0.58:2.56 (Figure S6, Supporting Information), which is in accordance with that of common metal divanadate $Co_3V_2O_8$. The elemental mapping images confirm that Co, V and O elements are evenly distributed in each shell (Figure 3c). The amorphous cobalt divanadate TSNBs are further annealed at 350 ºC for 2 h in air. The FESEM and TEM images reveal that the triple-shelled nanostructure is well maintained while the XRD pattern can be indexed to $Co_3V_2O_8$ (Figure S7, Supporting information). These results suggest that the cobalt polyvanadate in the outer shells are converted to cobalt divanadate during the

solvothermal treatment under neutral condition.[39] While the divanadate ions released from the outer shells further react with MOF inner cores to produce multi-shelled cobalt divanadate structures.

Importantly, the number of shells can be tuned by adjusting the temperature of the solvothermal process and the particle size of the MOF precursors. Specifically, cobalt divanadate nanoboxes with quintuple, quadruple and double shells (denoted as cobalt divanadate QuiSNBs, QuaSNBs and DSNBs respectively) are produced (Figure 3d-i; Figure S4b-d,f-h, Supporting Information) at the reaction temperature of 95 ºC, 75 ºC, and room temperature, respectively. In addition, the effect of particle size of ZIF-67 precursors on the number of shells of their derived cobalt divanadate nanoboxes is also investigated. After being heated at 95 ºC for 4 h, cobalt divanadate nanoboxes with quadruple and triple shells are produced using ZIF-67 precursors with the particle size of 430 and 300 nm (Figure S8 and S9, Supporting Information), respectively.

We then carry out the final ion-exchange process through the reaction of cobalt divanadate MSNBs with S^{2-} ions. The as-prepared cobalt divanadate multi-shelled particles can withstand the sulfidation process and subsequent annealing treatment at 350 ºC (**Figure 4**; Figure S10, Supporting information). As an example, the triple-shelled nanoboxes with sharp vertexes and rough surfaces can be clearly observed in magnified TEM images (Figure 4e,j). The SAED pattern shows multiple rings, indicating the polycrystalline feature (Figure S11, Supporting information). The XRD pattern of the obtained product can be well indexed to the CoS_2 phase (JCPDS card No. 41-1471; Figure S12, Supporting information).

The electrochemical properties of the cobalt sulfide multi-shelled nanoboxes are investigated as anode materials for SIBs. **Figure 5**a shows the charge-discharge voltage profiles of cobalt sulfide TSNBs, QuiSNBs, QuaSNBs and DSNBs for the second cycle at a current density of 500 mA g^{-1} within a voltage range of 0.01 to 3.0 V. In the discharge curves, the potential exhibits two poorly defined plateaus at ~1.7 V and ~0.9 V.[40-41] The discharge capacities of cobalt sulfide TSNBs, QuiSNBs, QuaSNBs and DSNBs are determined to be 478.1, 449.6, 442.2 and 380.0 mAh g^{-1},

respectively. As the electrode with the highest capacity, cobalt sulfide TSNBs are subjected to a cyclic-voltammetry (CV) test to investigate the mechanism of sodium storage in cobalt sulfide. The CV measurement at a scan rate of 0.1 mV s^{-1} within the potential window of 0.01-3 V is carried out (Figure S13, Supporting information). During the first discharge process, a wide reduction peak can be observed at ~0.64 V, corresponding to the reduction reaction between cobalt sulfide and sodium (Na), along with the formation of the solid-electrolyte interphase layer (SEI). In the following charge process, a strong oxidation peak appears at ~1.77 V, which could be attributed to the reverse oxidation reaction of Co to form CoS_x.[17, 42] In the following CV cycles, three individual reduction peaks and one pronounced oxidation peak are observed in each cycle. The profiles are overlapped well, suggesting good reversibility.

We further investigate the rate performance of the TSNBs at various current densities ranging from 0.1 to 5 A g^{-1} (Figure 5b). The electrode can deliver an average reversible capacity of 524, 481, 447, 422, 395, 346 mAh g^{-1} at the current densities of 0.1, 0.2, 0.5, 1.0, 2.0 and 5.0 A g^{-1}, respectively. In addition, a high specific capacity of 509 mAh g^{-1} is quickly recovered, when the current density is reduced back to 0.1 A g^{-1} from 5.0 A g^{-1}, suggesting the charge/discharge process is highly reversible. Of note, the TSNBs also possess higher capacity at each current density compared with three other samples (Figure S14a, Supporting information).

The cycling performance of the cobalt sulfide TSNBs is further investigated at different current densities. As presented in Figure 5c, the electrode can deliver a high discharge capacity of 695 mAh g^{-1} in the first cycle at a low current density of 200 mA g^{-1}, exhibiting a Coulombic efficiency of 68 %. The irreversible capacity for the initial cycle is mainly attributed to the formation of SEI layer.[13, 35] After that, the electrode delivers a capacity of 478 mAh g^{-1} in the second cycle and maintains a reversible capacity of 454 mAh g^{-1} after 100 cycles. The corresponding discharge-charge curves of the 2^{nd}, 3^{rd}, 5^{th}, 10^{th}, 50^{th} and 100^{th} cycles almost overlap with each other, indicating the electrochemical reactions are highly reversible and stable in the cobalt sulfide TSNBs electrode

(Figure S15, Supporting information). Through the cycling test, a high Coulombic efficiency around 99 % is obtained except for the first cycle. To study the potential effect of shell number on the sodium storage property, the cycling performances of the quintuple-, quadruple- and double-shelled samples are also investigated (Figure S14b, Supporting Information). A reversible capacity of 421, 398 and 395 mAh g^{-1} after 100 cycles at the current density of 200 mA g^{-1} is observed for quintuple-, quadruple- and double-shelled nanoboxes, respectively, which is lower than that of the triple-shelled sample. More over, TSNBs still remain a capacity of 438 mAg h^{-1} after 100 cycles at the current density of 500 mA g^{-1}, which is much higher than the values of the other three electrodes. (Figure S16, Supporting information). The sodium storage performance of these cobalt sulfide TSNBs is comparable to that of many reported cobalt sulfide-based anode materials (Table S1, Supporting information).[8, 13, 17-18, 41-46] The electrochemical impedance spectroscopy results reveal that the charge-transfer resistance of the cobalt sulfide TSNBs is smaller than that of the solid particles (Figure S17, S18, Supporting information). Although the multi-shelled structure is hard to be observed, the particles still retain their cubic morphology after 100 cycles (Figure S19). This observation suggests that multi-shelled nanostructures can better accommodate volume change to some extent and mitigate destruction of electrode materials during the repeated discharge-charge processes.

The enhanced performance of these cobalt sulfide multi-shelled nanoboxes might be attributed to their structural and compositional advantages. Specifically, the formation of interior multi-shelled nanostructures provides enhanced specific surface area and larger number of active sites for sodium storage. Next, the thin shells shorten the mass/charge transport pathway for the high-rate sodium insertion/removal. Finally, the gap between different shells provides the sufficient hollow space to overcome the large volume expansion during sodiation/desodiation process.

In summary, cobalt sulfide multi-shelled nanoboxes are fabricated through an ion-conversion-exchange strategy. Starting from cobalt-based MOF precursors, complex cobalt divanadate and cobalt sulfide multi-shelled particles with controllable number of shells are obtained through precise

manipulation of the designed ion conversion and exchange processes. Benefiting from the unique structure and composition, these cobalt sulfide multi-shelled particles exhibit enhanced electrochemical properties when evaluated as anode materials for sodium ion batteries. In particular, the triple-shelled nanoboxes can deliver a high specific capacity of 438 mAh g^{-1} after 100 cycles at a current density of 500 mA g^{-1}.

References

[1] T. Janoschka, N. Martin, U. Martin, C. Friebe, S. Morgenstern, H. Hiller, M. D. Hager, U. S. Schubert, *Nature* **2015**, *527*, 78.

[2] B. Dunn, H. Kamath, J.-M. Tarascon, *Science* **2011**, *334*, 928.

[3] N. Kittner, F. Lill, D. M. Kammen, *Nat. Energy* **2017**, *2*, 17125.

[4] J.-Y. Hwang, S.-T. Myung, Y.-K. Sun, *Chem. Soc. Rev.* **2017**, *46*, 3529.

[5] W. Luo, F. Shen, C. Bommier, H. Zhu, X. Ji, L. Hu, *Acc. Chem. Res.* **2016**, *49*, 231.

[6] M. S. Kim, E. Lim, S. Kim, C. Jo, J. Chun, J. Lee, *Adv. Funct. Mater.* **2017**, *27*, 1603921.

[7] P. K. Nayak, L. Yang, W. Brehm, P. Adelhelm, *Angew. Chem. Int. Ed.* **2018**, *57*, 102.

[8] S. Peng, X. Han, L. Li, Z. Zhu, F. Cheng, M. Srinivansan, S. Adams, S. Ramakrishna, *Small* **2016**, *12*, 1359.

[9] Y. Fang, X.-Y. Yu, X. W. Lou, *Adv. Mater.* **2018**, *30*, 1706668.

[10] C. Zhu, X. Mu, P. A. van Aken, Y. Yu, J. Maier, *Angew. Chem. Int. Ed.* **2014**, *53*, 2152.

[11] Z. Hu, Q. Liu, S.-L. Chou, S.-X. Dou, *Adv. Mater.* **2017**, *29*, 1700606.

[12] D. Su, S. Dou, G. Wang, *Adv. Energy Mater.* **2015**, *5*, 1401205.

[13] Y. Chen, X. Li, K. Park, L. Zhou, H. Huang, Y.-W. Mai, J. B. Goodenough, *Angew. Chem. Int. Ed.* **2016**, *55*, 15831.

[14] H. Park, J. Kwon, H. Choi, D. Shin, T. Song, X. W. Lou, *ACS Nano* **2018**, *12*, 2827.

[15] P. He, Y. Fang, X.-Y. Yu, X. W. Lou, *Angew. Chem. Int. Ed.* **2017**, *56*, 12202.

[16] Y. Fang, X.-Y. Yu, X. W. Lou, *Angew. Chem. Int. Ed.* **2018**, *57*, 9859.

[17] C. Wu, Y. Jiang, P. Kopold, P. A. van Aken, J. Maier, Y. Yu, *Adv. Mater.* **2016**, *28*, 7276.

[18] Y. Xiao, J.-Y. Hwang, I. Belharouak, Y.-K. Sun, *Nano Energy* **2017**, *32*, 320.

[19] G. Fang, Z. Wu, J. Zhou, C. Zhu, X. Cao, T. Lin, Y. Chen, C. Wang, A. Pan, S. Liang, *Adv. Energy Mater.* **2018**, *8*, 1703155.

[20] S. Chen, F. Wu, L. Shen, Y. Huang, S. K. Sinha, V. Srot, P. A. van Aken, J. Maier, Y. Yu, *ACS Nano* **2018**, *12*, 7018.

[21] B. Chen, H. Lu, J. Zhou, C. Ye, C. Shi, N. Zhao, S.-Z. Qiao, *Adv. Energy Mater.* **2018**, *8*, 1702909.

[22] B. Y. Guan, X. Y. Yu, H. B. Wu, X. W. Lou, *Adv. Mater.* **2017**, *29*, 1703614.

[23] B. Y. Guan, A. Kushima, L. Yu, S. Li, J. Li, X. W. Lou, *Adv. Mater.* **2017**, *29*, 1605902.

[24] B. Y. Guan, L. Yu, X. Wang, S. Song, X. W. Lou, *Adv. Mater.* **2017**, *29*, 1605051.

[25] B. Y. Guan, L. Yu, X. W. Lou, *Angew. Chem. Int. Ed.* **2017**, *56*, 2386.

[26] P. Zhang, B. Y. Guan, L. Yu, X. W. Lou, *Chem* **2018**, *4*, 162.

[27] X. Qi, W. Zheng, X. Li, G. He, *Sci. Rep.* **2016**, *6*, 33241.

[28] J. Qi, K. Zhao, G. Li, Y. Gao, H. Zhao, R. Yu, Z. Tang, *Nanoscale* **2014**, *6*, 4072.

[29] F. Qin, P. Cui, L. Hu, Z. Wang, J. Chen, X. Xing, H. Wang, R. Yu, *Mater. Res. Bull.* **2018**, *99*, 331.

[30] Y. Wang, L. Yu, X. W. Lou, *Angew. Chem. Int. Ed.* **2016**, *55*, 14668.

[31] J. Wang, N. Yang, H. Tang, Z. Dong, Q. Jin, M. Yang, D. Kisailus, H. Zhao, Z. Tang, D. Wang, *Angew. Chem. Int. Ed.* **2013**, *52*, 6417.

[32] S. Liu, W. Lei, Y. Liu, Q. Qiao, W.-H. Zhang, *ACS Appl. Mater. Interfaces* **2018**, *10*, 37445.

[33] Y. Von Lim, S. Huang, Y. Zhang, D. Kong, Y. Wang, L. Guo, J. Zhang, Y. Shi, T. P. Chen, L. K. Ang, H. Y. Yang, *Energy Storage Mater.* **2018**, *15*, 98.

[34] H. Hu, J. Zhang, B. Guan, X. W. Lou, *Angew. Chem. Int. Ed.* **2016**, *55*, 9514.

[35] H. Wang, C. Zhang, Z. Liu, L. Wang, P. Han, H. Xu, K. Zhang, S. Dong, J. Yao, G. Cui, *J. Mater. Chem.* **2011**, *21*, 5430.

[36] H. Hu, Bu Y. Guan, X. W. Lou, *Chem* **2016**, *1*, 102.

[37] X. Wang, L. Yu, B. Y. Guan, S. Song, X. W. Lou, *Adv. Mater.* **2018**, *30*, 1801211.

[38] Z. Q. He, P. M. Zhang, X. H. Zhang, L. Z. Xiong, S. X. Xiao, T. L. Chen, *Chem. World* **2001**. *4*, 206.

[39] A. Sigel, H. Sigel, *Metal Ions in Biological Systems*, CRC Press, **1995**.

[40] X. Liu, H. Liu, Y. Zhao, Y. Dong, Q. Fan, Q. Kuang, *Langmuir* **2016**, *32*, 12593.

[41] X. Liu, Y. Wang, Z. Wang, T. Zhou, M. Yu, L. Xiu, J. Qiu, *J. Mater. Chem. A* **2017**, *5*, 10398.

[42] Z. Chen, R. Wu, M. Liu, H. Wang, H. Xu, Y. Guo, Y. Song, F. Fang, X. Yu, D. Sun, *Adv. Funct. Mater.* **2017**, *27*, 1702046.

[43] J. S. Cho, J. M. Won, J.-K. Lee, Y. C. Kang, *Nano Energy* **2016**, *26*, 466.

[44] X. Liu, K. Zhang, K. Lei, F. Li, Z. Tao, J. Chen, *Nano Res.* **2016**, *9*, 198.

[45] H. Geng, J. Yang, Z. Dai, Y. Zhang, Y. Zheng, H. Yu, H. Wang, Z. Luo, Y. Guo, Y. Zhang, H. Fan, X. Wu, J. Zheng, Y. Yang, Q. Yan, H. Gu, *Small* **2017**, *13*, 1603490.

[46] F. Han, C. Zhang, B. Sun, W. Tang, J. Yang, X. Li, *Carbon* **2017**, *118*, 731.

Figures and captions

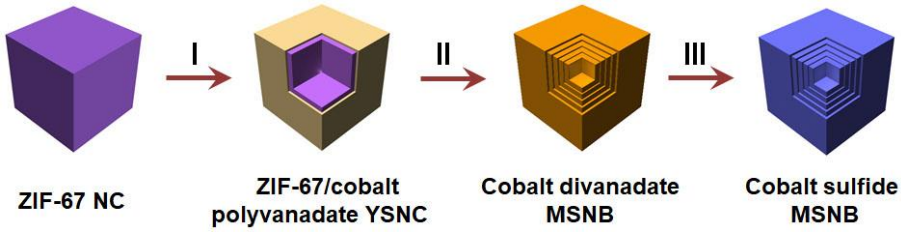

Figure 1. Schematic illustration of the formation process of cobalt sulfide MSNB: I) transformation of ZIF-67 NC to ZIF-67/cobalt polyvanadate YSNC through polyvanadate involved ion-exchange reaction in alkaline media; II) formation of cobalt divanadate MSNB via polyvanadate decomposition and *in situ* ion-exchange reaction between the released divanadate ions and ZIF-67 core; and III) formation of cobalt sulfide MSNB through a sulfidation reaction.

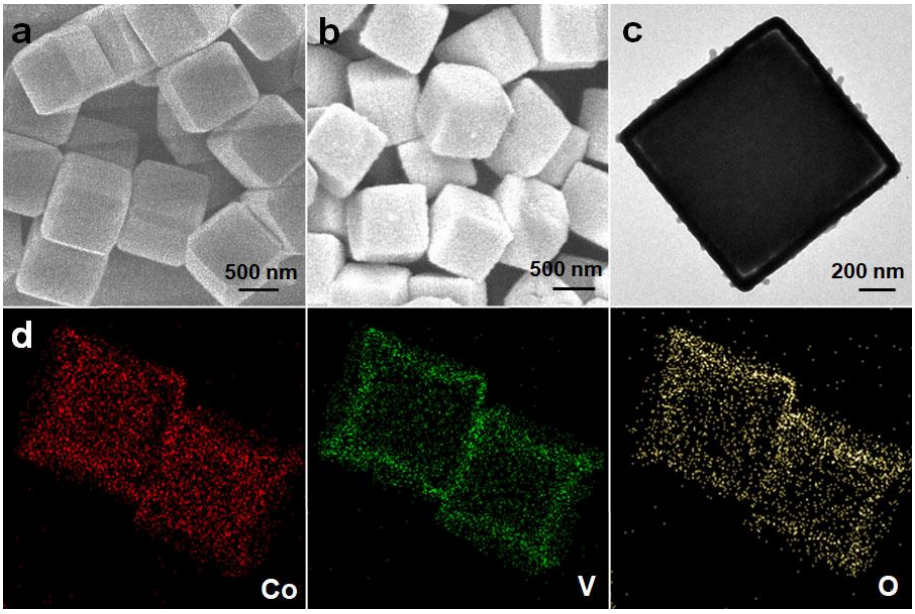

Figure 2. FESEM (a, b) and TEM (c) images of ZIF-67 NCs (a) and ZIF-67/cobalt polyvanadate YSNCs (b, c). (d) Element mapping images of ZIF-67/cobalt polyvanadate YSNCs.

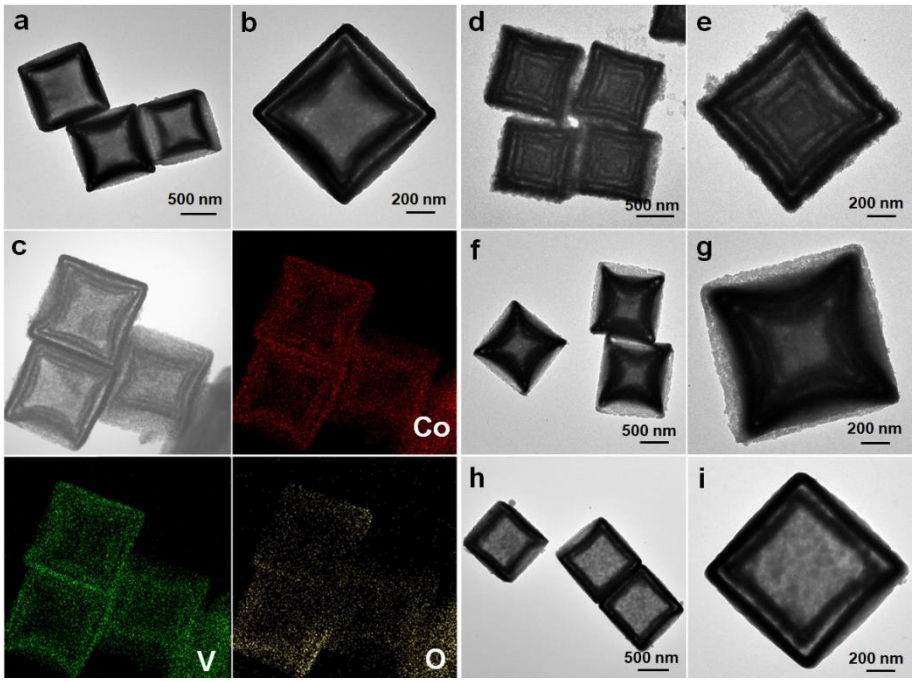

Figure 3. TEM (a, b, d-i) and element mapping (c) images of cobalt divanadate TSNBs (a-c), QuiSNBs (d, e), QuaSNBs (f, g), and DSNBs (h, i).

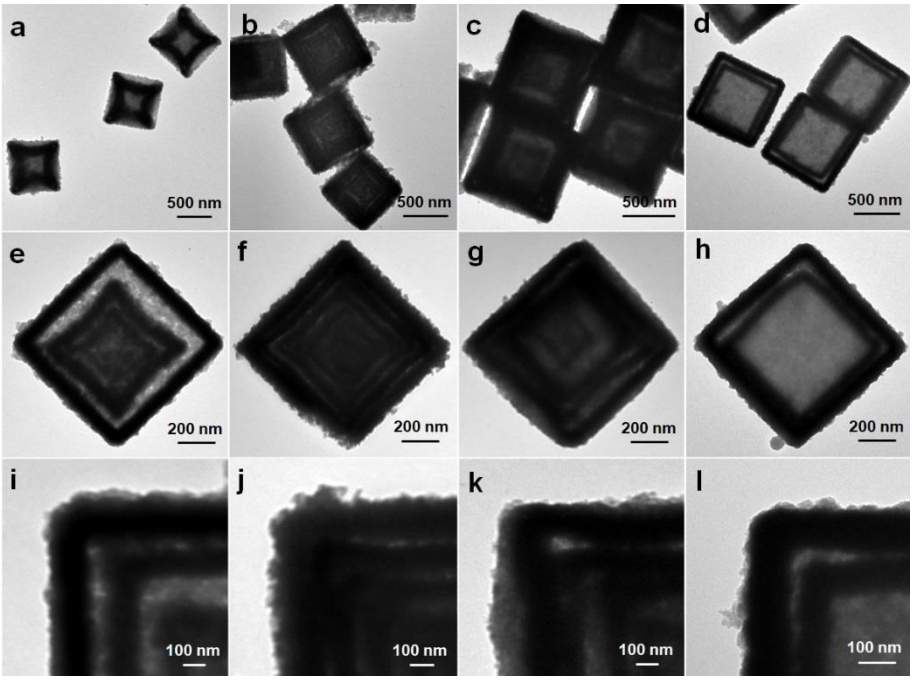

Figure 4. TEM images of cobalt sulfide TSNBs (a,e,i), QuiSNBs (b,f,j), QuaSNBs (c,g,k) and DSNBs (d,h,l).

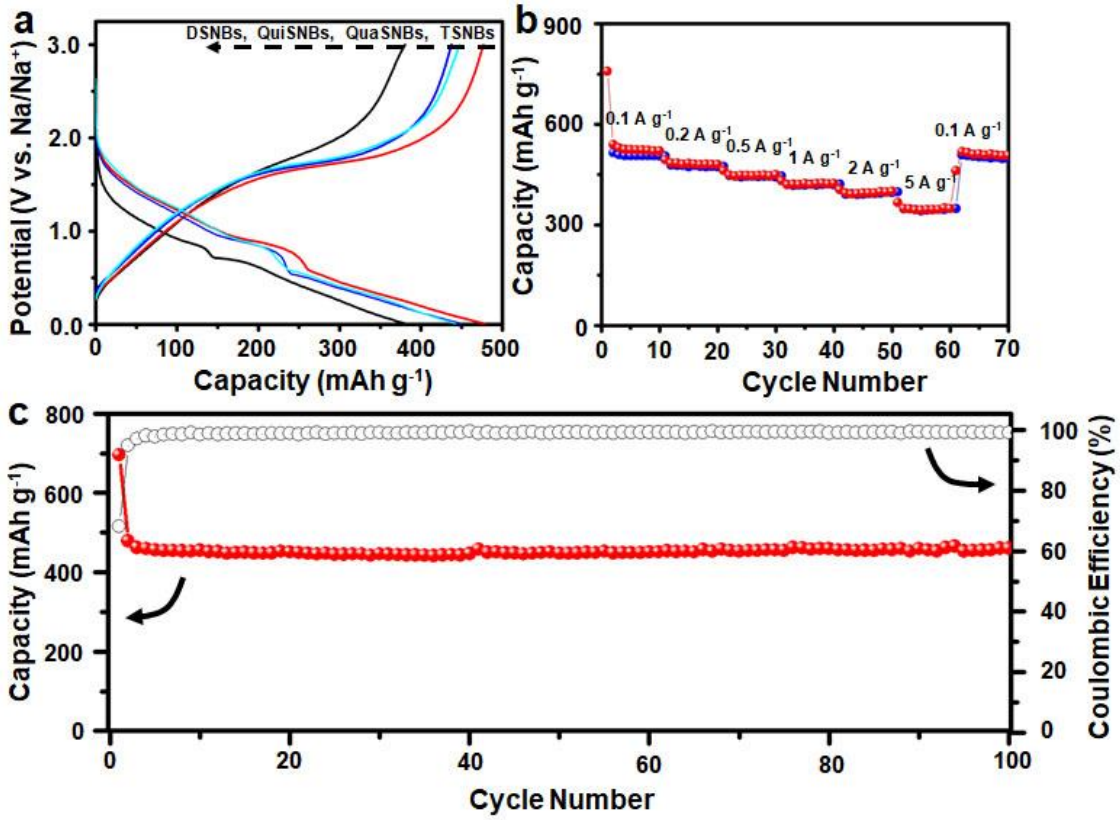

Figure 5. (a) The discharge-charge voltage profiles of cobalt sulfide MSNBs with different shell numbers for the second cycle at the current density of 500 mA g^{-1}. (b) The rate performance of cobalt sulfide TSNBs at various current densities and (c) cycling performance for 100 cycles at the current density of 200 mA g^{-1}.

for Table of Content Entry

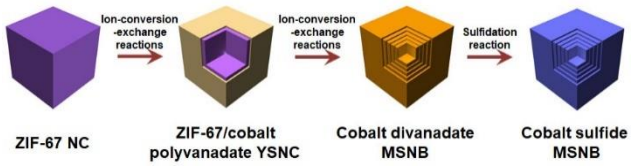

Cobalt sulfide multi-shelled nanoboxes are prepared through an ion-conversion-exchange strategy. With the structural and compositional advantages, these unique cobalt sulfide multi-shelled nanoboxes exhibit enhanced sodium storage performance when evaluated as anodes for sodium-ion batteries.